

1 **Title:** Urban food forestry transforms fine-scale soil function for rapid and uniform carbon
2 sequestration.

3 **Author Information:**

4 Brad Oberle¹†¹

5 Steven Bressan^a

6 Joseph McWilliams^{a,b}

7 Erika Díaz-Almeyda^a

8 ^aDivision of Natural Sciences, New College of Florida, 5800 Bay Shore Road, Sarasota FL

9 34243, USA

10 ^bFaculty of Humanities, University of Hamburg, Edmund-Siemers-Allee 1, 20146 Hamburg,

11 Germany

12 †To whom correspondence should be addressed, boberle@ncf.edu

13 ¹<https://orcid.org/0000-0002-4227-3352>

14 **Word Count:** 8513

15

16 **Acknowledgements**

17 Meghan Midgley, Joshua Breithaupt and Richard Hauer provided insightful comments on an
18 early draft of this manuscript. An anonymous reviewer made excellent suggestions for improving
19 the comparison between land cover types. Deniz Wilson and Deric Harvey completed informal
20 surveys of the lawn habitat. New College of Florida students funded the land use experiment
21 through the New College of Florida Green Fee. Additional funds for soil analyses were provided
22 by the New College of Florida Foundation.

23 **Abstract**

24 Urbanization displaces agriculture and natural ecosystems, constraining food security and carbon
25 (C) sinks. A proposed solution, Urban Food Forestry (UFF), promises local food from trees that
26 can sequester C faster than other land cover types as long as soil function can sustain increased
27 above and belowground productivity . We compared fine-scale variation in soil physical,
28 chemical and biological properties within and between UFF and traditional lawn for evidence of
29 changes in belowground ecosystem services. Both land covers sequestered C, but UFF did so
30 834% faster, especially in upper soil strata where soil bulk density fell by 50% and microbial
31 activity increased by 1167% . Species richness of both soil fungi and bacteria increased along
32 with nutrient concentrations. Contrary to expectations, that different tree traits would drive
33 increasing fine scale variability in C density, soils beneath the UFF became more uniform, which
34 is consistent with the rapid emergence of system-level regulation. Soil C mass balance may
35 distinguish forests from collections of trees and determine how long UFF helps cities store their
36 carbon and eat it too.

37 **Keywords:** agroforestry, carbon sequestration, permaculture, soil function, urban agriculture

38 **Introduction**

39 Both population growth and anthropogenic warming are concentrated in cities. Emerging
40 solutions to these related issues reimagine where and how to grow food. Relocating production
41 to underutilized urban areas like vacant lots and lawns can increase yields (McDougall et al.
42 2019) while reducing greenhouse gas emissions (Cleveland et al. 2017). Further incorporating
43 useful trees diversifies agricultural outputs while storing more C in wood and soils (De Stefano
44 and Jacobson 2018). Combining the high provisioning services of urban agriculture with the
45 climate regulating services of agroforestry may be possible in Urban Food Forests (UFF). Clark
46 and Nicholas (2013) defined UFF as “the intentional and strategic use of woody perennial food
47 producing species in urban edible landscapes to improve the sustainability and resilience of
48 urban communities.” Because this broad definition includes isolated trees, other authors
49 emphasize a more systems-based approach by stipulating that UFF should further mimic the
50 structural and functional complexity of natural forests where diverse perennials grow together
51 (Salbitano et al. 2019). Early assessments of UFF are promising. A mature 1 ha food forest can
52 feed 5-6 people per year (Nytofte and Henriksen 2019) while sequestering 40,000 kg of C in
53 living plant tissues (Schafer et al. 2019). Whether or not UFF can approximate the C dynamics of
54 other forest ecosystems while maintaining yields remains unknown.

55 A major factor that could limit services from UFF is soil function. Soils supply roots with
56 key resources and provide a medium for interactions with microbial symbionts and pathogens.
57 Moreover, soils can store C in more chemically stable forms than living vegetation (Trumbore
58 2000). However, the physical, chemical and biological properties of both urban and agricultural
59 soils tend to reduce a range of soil functions (Cardoso et al. 2013). Urban soil compaction limits
60 root growth and water availability (Nawaz et al. 2013). Whether or not trees planted in UFF can

61 either tolerate or reverse compaction remains unknown. Furthermore, urban and agricultural soils
62 can have low microbial diversity and activity, which could limit nutrient availability and C
63 cycling (Guilland et al. 2018; Díaz-Vallejo et al. 2021). Finally, UFF explicitly incorporates
64 woody species with contrasting functional traits, which could change fine-scale soil properties
65 relative to more homogenous land cover types, like lawns.

66 To understand how belowground changes support ecosystem services from UFF, we
67 analyzed fine-scale variation in soil structure and function in an urban land use experiment. The
68 New College Food Forest and Carbon Farm is a small (0.057 ha) demonstration UFF in a rapidly
69 urbanizing area of Florida, U.S.A. Shortly after installation in 2017, we measured soil C at 56
70 locations across the UFF and adjacent lawn in different vertical strata. We compared C
71 measurements using a novel before-after impact-control (BACI) design that incorporated
72 uncertainty from calibration curves while controlling for spatial autocorrelation in a hierarchical
73 Bayesian framework. Our research objectives were to (1) document differences in physical,
74 chemical and biological aspects of soil function between UFF and adjacent lawn and (2) to
75 analyze fine-scale variation in soil C sequestration within and between land cover types. We
76 expected that conversion to UFF would improve soil function by decompacting soils and
77 increasing nutrient concentrations, microbial activity and richness relative to lawns, which had
78 experienced consistent, low-intensity management for at least 70 years. Furthermore, we
79 expected to observe higher rates of soil C sequestration beneath UFF, with increasing spatial
80 variation driven by contrasting tree traits.

81 **Methods**

82 *Site Description*

83 The land use experiment took place on the New College of Florida Campus at
84 [27.380446°N, -82.562416°W] in southwestern Florida approximately 100 m east of Sarasota
85 Bay and 600 m west of the Sarasota-Bradenton International Airport. The climate is humid
86 temperate-subtropical with mean annual temperature of 22.8°C and annual precipitation of 1346
87 mm varying between a hot summer wet season and a cool winter dry season. Local soils are Eau
88 Galle - Myakka Fine Sands, with sandy and loamy marine deposits as the main parent materials
89 (Soil Survey Staff, 2023). Prior to urbanization, the predominant land cover types in the area
90 were pine flatwoods, a savannah-like ecosystem maintained by periodic fire with a discontinuous
91 canopy of *Pinus elliottii*, a dense shrub layer dominated by *Serenoa repens*, and a rich mixture of
92 grasses and forbs (Sparkman and Bryant, 2016). In 1921, the study area was developed by a real
93 estate mogul who constructed an estate with two major buildings and roadways. By 1948, when
94 the oldest aerial imagery that is available today was captured (USDA 1948), several large pines
95 remained but the groundcover on the property was more uniform than surrounding undeveloped
96 parcels, consistent with conversion to lawn (Figure S1). Lawn management in the United States
97 typically promotes uniform cover by desirable species of grasses by some combination of
98 periodic mechanical mowing, irrigation, and nutrient enrichment while controlling undesirable
99 species with herbicide, fungicide or pesticides (Thompson and Kao-Kniffin 2019).

100 The establishment of the UFF began in February 2016 with sheet mulching over the
101 existing lawn. Community volunteers then combined locally sourced topsoil, compost and
102 biochar into berms that were approximately 10 cm high and 1 m wide. Starting in May 2016,
103 students planted 50 seedlings representing 33 different useful woody species (Table S1) into

104 rows along the berms along with assorted short-lived woody and pseudo-woody plants, vines,
105 and herbaceous plants. Ongoing maintenance consisted of watering, trail-making, mulching and
106 spreading compost generated by students on campus from food scraps. During this period, the
107 adjacent lawn area was mowed biweekly at a 6 - 12 cm height, retraining clippings to the turf and
108 without irrigation or chemical fertilizer application. An informal survey of plants present in lawn
109 habitats identified 36 species, with grasses (Poaceae) being the most diverse plant family,
110 represented by at least 8 different taxa. The most frequently encountered species in the footprint
111 of the study area were the common turfgrass, *Paspalum notatum* Flügge (Poaceae), and the
112 introduced subshrub, *Sida acuta* Burm.f. (Malvaceae) (unpublished data).

113 *Sampling design*

114 To understand how implementation affected soil function, we employed a novel Before-
115 After-Control-Impact (BACI) sampling design. Originally developed to estimate the
116 environmental effects of unique interventions, BACI compares the magnitude of change in
117 repeated measurements before and after implementation to similar measurements at a control
118 location while statistically controlling for autocorrelation from non-random sampling (Conner et
119 al. 2015). We applied different aspects of the BACI design to our different research objectives.
120 For our primary research objective, which was to quantify fine-scale variation in C sequestration,
121 we established impact and control sampling arrays in the UFF and adjacent lawn, respectively.
122 We use fixed landmarks to collect soil samples at 4 m intervals along each berm for 28 sampling
123 locations in a hexagonal array, which we reproduced in the lawn. We sampled soils in both
124 arrays shortly after construction in 2017 and after two years of managing the UFF in 2019. We
125 controlled for spatial autocorrelation using a hierarchical Bayesian model (see Supplementary
126 Methods).

127 In addition to representing spatial variation in the horizontal dimensions, we also
128 analyzed changes across vertical strata. At each sampling location and time interval, we removed
129 herbaceous vegetation and detritus and then used a gauge auger to extract a soil core. In the UFF,
130 we split the upper 30 cm of each core into three vertical strata representing the berm stratum of
131 imported soils (0-10 cm), the upper stratum of original lawn soils (10-20 cm) and the lower
132 stratum of original lawn soils (20-30 cm) ($n=84$). In the lawn, we only sampled the top 20 cm of
133 soils and split samples into two strata (0-10 cm and 10-20 cm, $n=56$). Berm soils should show
134 the greatest impact effect, followed by the original upper stratum and finally the original lower
135 stratum compared to the corresponding control strata in the lawn.

136 For the secondary research objective, comparing other physical, chemical and biological
137 differences we only sampled after implementation in 2019 but again compared measurements
138 between the impact and control areas using a spatial model to account for autocorrelation. In
139 each area, we added four sampling sites that corresponded to an expanded margin of the UFF
140 and an equivalent area of the lawn for 64 sampling locations. At all locations, we measured soil
141 bulk density (SBD) in every stratum ($n=160$). We also measured soil respiration at every location
142 and stratum except for the lowest ($n=96$).

143 For soil nutrients and microbial diversity, we used different sampling approaches. In a
144 random subset of 20 sites from each area, we collected additional soil samples that we physically
145 aggregated and analyzed for soil nutrient concentrations. Finally, we leveraged preliminary
146 results from the soil C analysis to identify six sampling locations—four in the UFF and two in
147 the lawn—from which we remeasured soil nutrients along with microbial diversity. For a
148 summary of the sampling strategy for each dataset and analysis, refer to Table S2.

149 *Soil C measurements, calibration and projection*

150 During the 2017 campaign, we air-dried all 140 samples to constant weight and analyzed
151 them for organic carbon (OC) content (%) using chromic acid wet oxidation (Walkley and Black
152 1934). During the 2019 campaign, we transferred all 160 samples to sealed polyethylene bags for
153 storage up to two days at 4°C. After measuring soil respiration from a subset of samples, we
154 dried samples to 105°C for a minimum of 8 hours and calculated Soil Bulk Density (SBD) as the
155 ratio of sample dry mass to fresh volume. We then measured soil organic matter via loss on
156 ignition (LOI). Specifically, we combusted up to 15 mL of dried sample for 4 hours at 550°C in
157 a Lindberg Blue M muffle furnace (Fisher Scientific, Waltham MA). We calculated LOI as the
158 ratio of the combusted sample mass to its initial dry mass.

159 Because we measured different but related variables in each sampling campaign (OC in
160 2017; SBD and LOI in 2019), we generated calibration relationships using a stratified dataset. In
161 2019, we collected an additional 15 samples representing the highest, lowest, and approximate
162 mean LOI from each stratum and area, where we measured SBD and LOI using the methodology
163 described above and Walkley-Black OC using the same analytical lab as in 2017 (Figure S2). To
164 identify the most adequate calibration relationships, we used the function “lm” in R-package
165 “stats” to fit pairwise regressions between original and log-transformed values of OC and LOI as
166 well as between SBD and OC while including every combination of area, stratum and their
167 interactions as covariates. We selecting the functional form of the relationship with the lowest
168 AIC (Table S3) for further analysis.

169 Uncertainty from calibration curves and spatial autocorrelation are common in soil C
170 analyses and BACI designs (Conner et al. 2015). To address each of these complications in a
171 coherent statistical framework, we used a Hierarchical Bayesian (HB) approach. HB models are
172 modular and integrate uncertainty from multiple sources into posterior distributions of key

173 quantities (Ogle and Barber 2012). We describe the model in detail in Supplementary Methods
 174 S1, which also includes all code and data necessary to reproduce the analysis. We note that this
 175 approach tends to broaden credible intervals without biasing the means. Therefore, estimates of
 176 the statistical significance of differences between land cover types and years are conservative
 177 relative to conventional analyses that would use calibration constants, censor observations or
 178 ignore spatial autocorrelation.

179 To estimate the attainable SOC stocks in the UFF, we used fine-scale variation in C
 180 sequestration rates to parameterize a simple mass balance equation for SOC (Morais et al. 2019).
 181 The model assumes that the change in SOC depends on the difference between the SOC input
 182 (K) and the mineralization rate (α):

$$183 \quad \frac{dSOC}{dt} = K - \alpha * SOC \quad (\text{Eq. 1})$$

184 We calculated these quantities in the UFF by applying the moment-based estimators for
 185 the intercept and slope parameters to the spatially detrended estimates of SOC in 2017 and 2019
 186 across all ($o=1 \dots 28$) sampling locations (See Supplementary Methods, Eq. S1-S8):

$$187 \quad \alpha = \frac{Cov(SOC17_o, SOC19_o - SOC17_o)}{Var(SOC17_o)} \quad (\text{Eq. 2})$$

$$188 \quad K = \overline{SOC19_o - SOC17_o} - \alpha * \overline{SOC17_o} \quad (\text{Eq. 3})$$

189 In addition to using these values as estimates for SOC input and mineralization in the
 190 UFF, we projected SOC accumulation through time to its equilibrium value (K/α) using the
 191 solution to the differential equation:

$$192 \quad SOC(t) = \frac{K}{\alpha} (1 - e^{-\alpha t}) + e^{-\alpha t} * \overline{SOC17_o} \quad (\text{Eq. 4})$$

193 where t is time in years. To relate the quantities from the Mass Balance Equation (Eq. 1) to
 194 system level regulation of the UFF, we estimated the minimum quantity of mulch necessary to
 195 meet the estimated C supply rate (K). Specifically, we used the standard C content of wood of

196 50% (w/w) (USDA 2011) and bulk density of dry wood chips of 200 kg m^{-3} (Forest Products
 197 Laboratory 2010) to convert supply rate estimates into mass and depth of mulch.

198 To propagate uncertainty from all aspects of the model, including calibration curve
 199 estimation (Supplementary Methods Eq. S1, S3, S7, S9), and spatial detrending (e.g.
 200 Supplementary Methods Eq. S5, S6), we calculated the SOC input and mineralization parameters
 201 (Eq. 1) during Markov Chain Monte Carlo (MCMC) sampling and drew 1200 samples from the
 202 MCMC chains for the projection (Eq. 4). For details of model fitting, see Supplementary
 203 Methods.

204 *Soil respiration*

205 We measured soil respiration in 2019 as the mass specific respiration rate (MSRR) under
 206 standard laboratory conditions. Within 48 hours of collection, we allowed samples to equilibrate
 207 to room temperature inside 500 ml glass tissue culture flasks, which served as static respiration
 208 chambers. We measured initial headspace CO_2 concentrations by injecting 10 mL of soda-lime
 209 scrubbed air and pumping the syringe three times to mix. We measured the resulting 10 mL
 210 headspace sample using a PP Systems EGM-4 Infrared Gas Analyzer (Amesbury, MA) and then
 211 repeated the procedure after an incubation of approximately 20 minutes. We calculated the
 212 headspace C masses by applying the ideal gas law:

$$213 \quad \text{mass C} = 12.05 * \text{PPM} \frac{\text{pressureATM} * (\text{jarVolume} - \text{coreLength} * \pi * \text{augerRadius}^2)}{(273.15 + \text{labTemp}) * R} \quad (\text{Eq. 5})$$

214 Where $R = 82.05 \text{ cm}^3 \text{ atm g}^{-1} \text{ mol}^{-1} \text{ K}^{-1}$. We then calculated MSRR as the increase in headspace C
 215 $\text{min}^{-1} \text{ g}^{-1}$ of dry soil.

216 To assess the biological relevance of differences in SBD and MSRR between upper strata
 217 of the lawn and UFF in 2019, we quantified the frequencies with which samples exceeded US
 218 Department of Agriculture thresholds for each soil health metric (Soil Science Division Staff,

219 2017). Soil compaction limits plant growth in sandy soils with bulk densities greater than 1.6 g
220 cm^{-3} and in sandy loams with bulk densities greater than 1.4 cm^{-3} . Those with respiration rates
221 below 0.032 $\mu\text{g C min}^{-1} \text{g}^{-1}$ are considered to have very low soil activity relative to a typical
222 value of 0.056 $\mu\text{g C min}^{-1} \text{g}^{-1}$ in agricultural soils.

223 *Soil nutrients and microbes*

224 To represent differences in soil nutrients, we air dried samples and mailed them to the
225 University of Georgia Soil, Plant, and Water Laboratory for quantification of soil pH,
226 phosphorus (P), potassium (K), calcium (Ca), magnesium (Mg), zinc (Zn), manganese (Mn), iron
227 (Fe), copper (Cu), molybdenum (Mo) and cation exchange capacity (CEC) by Mehlich I sum
228 with percent base saturation. We summarized variation in scaled nutrient concentrations using
229 Principal Component Analysis (PCA) using the function “prcomp” in R v 4.0.2 packages “stats.”
230 (R Core Team 2020).

231 To describe soil microbial diversity, we collected six total samples using the stratified
232 approach described above. At each location, we collected five cores to 20 cm depth with a
233 sterilized gauge auger. After removing the top 5 cm, the soil was homogenized and frozen at -80
234 °C. DNA was extracted using a Qiagen DNeasy PowerSoil kit (Qiagen USA, Germantown, MD)
235 following the standard protocol except for increasing the vortexing time to 10 min to improve
236 inhibitor removal. DNA was extracted into 100 μL nanopure water. We sent 25 μL of total DNA
237 to Molecular Research LP Laboratory (MR DNA, Shallowater, TX) for diversity assays based on
238 DNA barcoding. For bacteria identification, 16S rRNA V4 region was amplified (515/806
239 primers, Parada et al. 2016) with a HotStar Taq Plus Master Mix Kit following manufacturer
240 instructions (Qiagen, USA). For fungal identification, the ITS region was amplified (ITS1 and
241 ITS4 primers, White et al., 1990). Amplicons were barcoded using bTEFAP (Dowd et al., 2008),

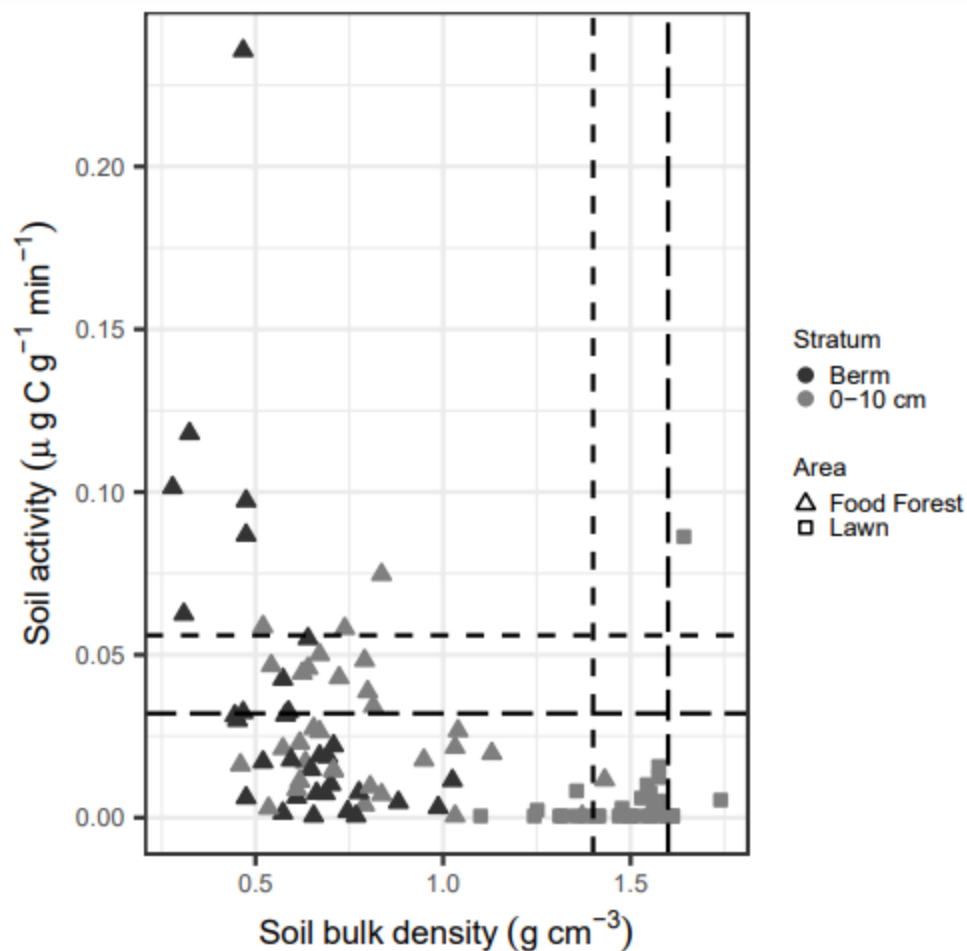
242 adapted for the sequencing technology used here. Sequencing was performed with ThermoFisher
243 Scientific Ion S5, following manufacturers' instructions. Sequences were processed by removing
244 barcodes, primers, short sequences <150 bp, sequences with ambiguous base calls and sequences
245 with homopolymer runs exceeding 6bp. Then sequences were denoised, OTUs were generated
246 by clustering at 97% similarity (3% divergence), and singleton sequences and chimeras were
247 removed. The resulting OTUs were taxonomically classified using BLASTn against a curated
248 database. The number of sequences per taxonomic level were compiled as counts.

249 We calculated observed richness and the Chao 1 alpha diversity metric from fungal and
250 bacterial samples using the function "estimate_richness" in the R package phyloseq (McMurdie
251 and Holmes 2013) and considered areas different if their estimated standard errors did not
252 overlap. To represent overall differences in community composition, we used Principal
253 Coordinate Analysis (PCoA) of Bray-Curtis distances implemented using "ordinate" in phyloseq.
254 To identify distinctive fungal taxa in each area, we used indicator species analysis as
255 implemented by the "multipatt" function in R package "indicspecies" (De Cáceres and Legendre
256 2020), correcting for differences in sample numbers in each area. We selected any taxa with
257 marginally significant point biserial correlation coefficients ($p < 0.1$) for further functional
258 characterization by cross referencing fungal OTUs to the FunGuild Database (Nguyen et al.
259 2016). We analyzed evidence for functional differentiation by comparing the trophic guild
260 classification of distinctive fungal OTUs in the UFF versus all others using Fisher's Exact Test
261 in R package "stats".

262 **Results**

263 Converting lawn to UFF precipitated a dramatic change in soil structure and function
264 after only two years (Fig. 1). The majority of samples from the top 10 cm of lawn soil (24/32)

265 exceeded the soil compaction standard for sandy loams ($>1.4 \text{ g cm}^{-3}$) and five samples exceeded
266 the soil compaction standard for sands ($>1.6 \text{ cm}^{-3}$). In contrast, just 1/32 samples from the same
267 stratum beneath the UFF exceeded 1.4 cm^{-3} , despite the added weight of plants and soils on
268 berms. Taking the spatial structure of the sampling locations into account, the average SBD of
269 the upper stratum of the lawn was 1.478 g cm^{-3} ([1.435, 1.521] 95%CI), which was nearly double
270 that of the corresponding stratum beneath the UFF, 0.751 g cm^{-3} ([0.689, 0.820] 95%CI). The
271 differences in the original lower strata were less extreme but still significantly lower under the
272 UFF (Lawn 10-20 cm mean SBD= 1.336 g cm^{-3} [1.297, 1.375] 95% CI, UFF original 10-20 cm
273 mean SBD= 0.969 g cm^{-3} [0.885, 1.058] 95%CI). The lowest average SBD occurred in the
274 imported soils in the berm stratum of the UFF (mean SBD= 0.583 g cm^{-3} [0.534, 0.637] 95%CI).



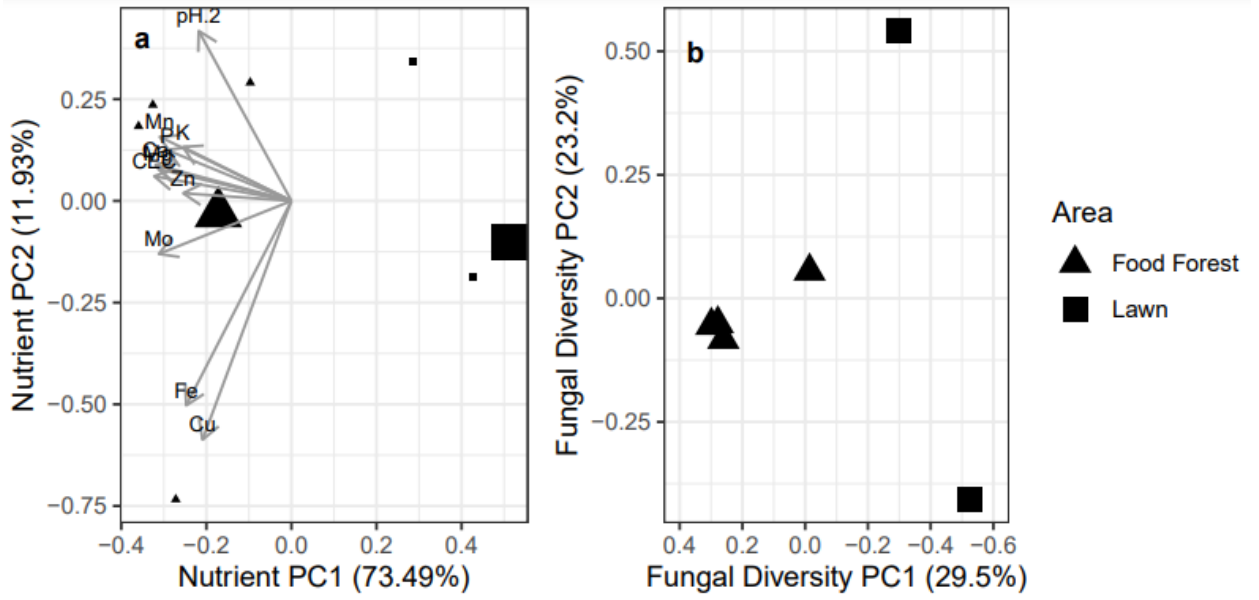
275
 276 **Fig. 1** Urban food forest soils were more active and less compacted than lawn soils. Dashed lines
 277 correspond to agronomically relevant soil function thresholds (see Materials and Methods) with
 278 long dashes corresponding to the least functional range, and short dashes corresponding to
 279 intermediate function. Triangles correspond to samples from the Urban Food Forest and squares
 280 to samples from the lawn. Dark fill indicates samples from the imported berm stratum in the
 281 Urban Food Forest. Light fill corresponds to the original soil strata in either area

282 Rapid soil decompaction in the UFF was associated with an agriculturally relevant
 283 increase in microbial activity (Fig. 1). Taking the spatial structure of the 32 sampling locations
 284 into account, the average mass specific respiration rate in the upper stratum of lawn soil was
 285 0.0015 μg C g⁻¹ min⁻¹ ([0.0012, 0.0019] 95%CI), approximately 20 times slower than the

286 common threshold for the least healthy category of soil microbial activity of $0.032 \mu\text{g C g}^{-1} \text{min}^{-1}$
287 ¹. In the corresponding stratum under the UFF, average respiration rates were an order of
288 magnitude faster, $0.0175 \mu\text{g C g}^{-1} \text{min}^{-1}$ ([0.0112, 0.0260] 95%CI) and similar to the respiration
289 rate of berm soil ($0.0156 \mu\text{g C g}^{-1} \text{min}^{-1}$ [0.0100, 0.0230] 95%CI). Among 64 UFF samples, 21
290 exceeded the threshold for the least healthy category of soil activity compared to just one sample
291 of 32 from the lawn. Among all 96 samples, 11/12 with healthy levels of soil activity ($>0.056 \mu\text{g}$
292 $\text{C g}^{-1} \text{min}^{-1}$) occurred in the UFF.

293 Compared to control sites in the lawn, UFF soils also had higher concentrations of soil
294 nutrients (Fig. 2A). Cation exchange capacity (CEC), which measures overall nutrient
295 availability, was only 7.75 meq per 100g in a physically aggregated sample from the lawn. In
296 contrast, CEC in the UFF was 4.63 times higher. Every measurement of K, Ca, Mg, Mn and Fe
297 concentrations from the five UFF samples exceeded those from the three lawn samples.

298



299

300 **Fig. 2** Urban food forest soils have higher nutrient concentrations (a) and distinctive fungal
 301 communities (b) compared to lawn soils. Large symbols in panel (a) correspond to physically
 302 aggregated samples from each area. Small symbols in panel a correspond to 6 additional
 303 stratified samples. Triangles correspond to samples from the Urban Food Forest and squares to
 304 samples from the lawn.

305

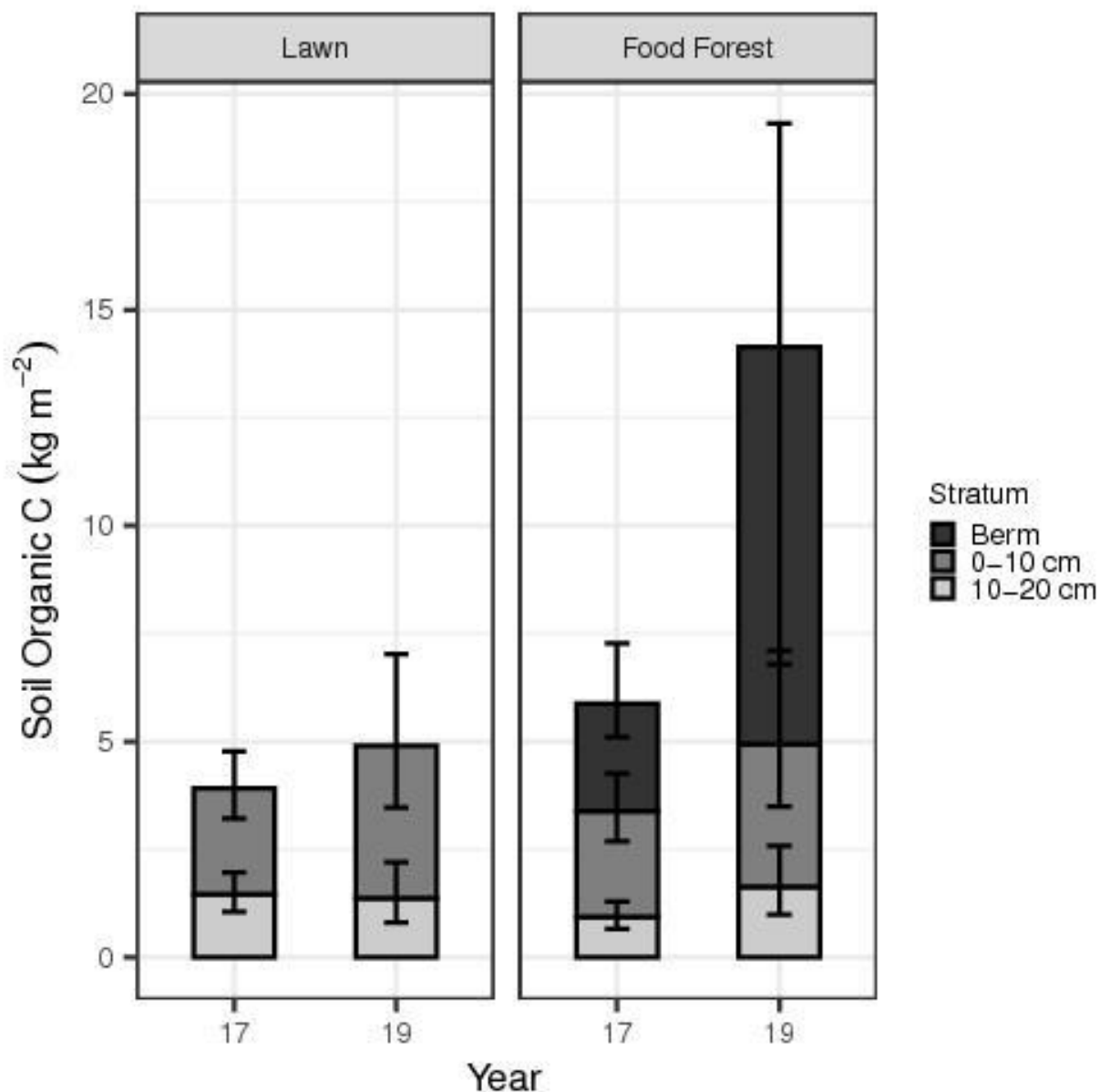
306

307 Microbial communities from more functional UFF soil were diverse and distinctive
308 compared to lawn soil (Fig. 2B). Among 417 unique fungal OTUs, the Chao 1 index of the four
309 UFF samples was 423.1 (\pm 4.4 s.e.) compared to 395.3 (\pm 18.5 s.e.) in two samples from the
310 lawn. Overall, 99 OTUs were unique to the UFF compared to just 24 from the lawn. The UFF
311 included 26 marginally significant indicator taxa that matched the FunGuild traits database. The
312 trophic modes for the 26 distinctive UFF soil fungi were significantly different from 224 other
313 fungi (Fisher's Exact Test, $p=0.012$). Fungal communities exhibited fine scale variability, with
314 different taxa dominating specific samples (Supplemental Table S4 A). For example,
315 *Trechispora* was the most abundant taxon in one UFF soil sample (16.95%) and was present at
316 low abundance in the rest of the samples (0.04-0.09%). Similarly, *Pisolithus* was the most
317 abundant taxon present in a lawn sample (29.82%) but was present at low abundance in the rest
318 of the samples (0.08-0.13%).

319 Bacterial communities from the UFF were also more diverse and distinctive. Among
320 2323 bacterial OTUs, the Chao 1 index for the UFF samples was 2317.5 (\pm 10.7 s.e.) with 130
321 unique taxa compared to an alpha diversity of 2291.3 (\pm 19.4 s.e.) and 39 unique taxa in the lawn.
322 The most abundant bacterial taxa in each sample were variable with some overlap between UFF
323 samples and the lawn samples (Supplemental Table S4,B). *Steroidobacter* were the most
324 abundant bacteria in UFF soils (1.40-4.91%) compared to the lawn soils (0.17-1.24%). This
325 genus has been previously reported present in farmed soils (Huang et al. 2019). *Holophaga*,
326 which has been reported from natural forest soils (Hackl et al. 2004), was also abundant in UFF
327 soils (1.18-2.89%) but had low abundance in lawn soil (0.06-0.42%). The most abundant genus
328 in the lawn soil was *Actinoallomurus*, which was reported present in mangrove soils (Tang et al.
329 2013), however it was found in small amounts (2.4%).

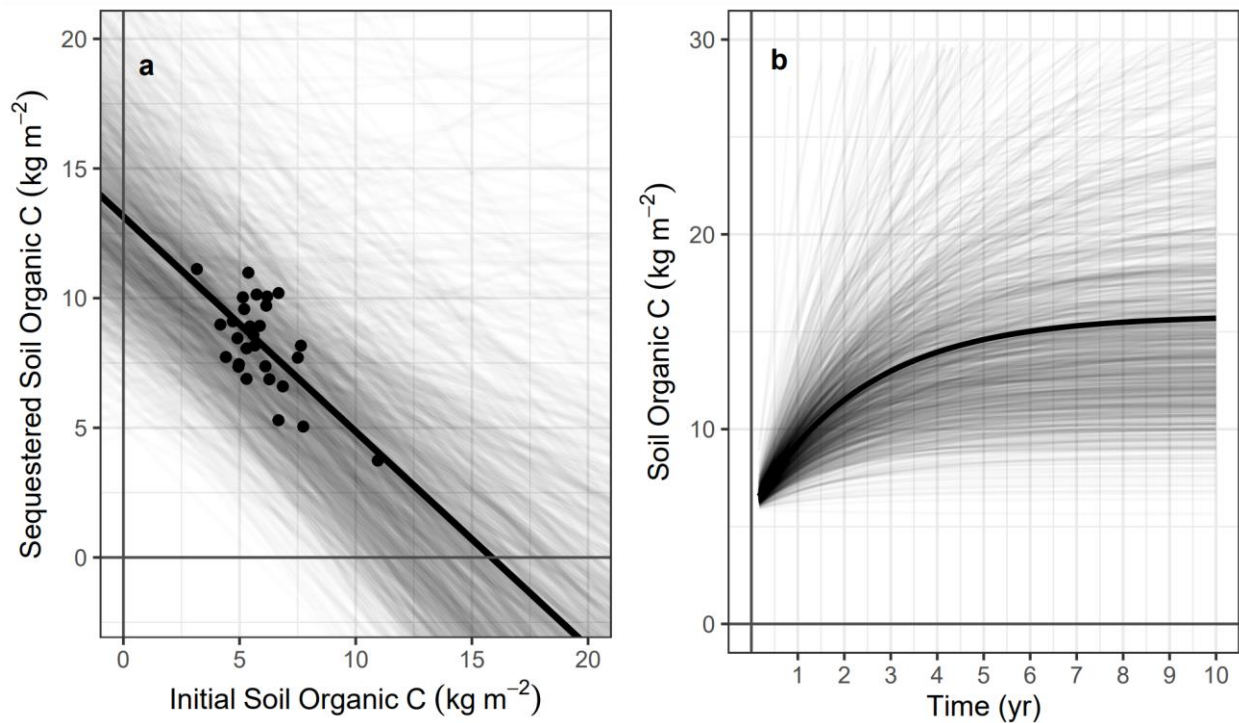
330 As soil functions improved, and distinctively rich microbial communities developed, the
331 UFF sequestered much more organic C belowground than traditionally managed lawn. Shortly
332 after establishment, all of the difference in SOC stocks between areas was attributable to C added
333 with the berm stratum (Fig. 3). After two years of management for useful tree growth, SOC more
334 than doubled among 168 samples from the top 30 cm of the UFF. Taking the spatial structure
335 into account, the average soil C concentration in the UFF increased from 5.88 ([4.48, 7.65]
336 95%CI) to 14.14 ([8.94, 22.28] 95%CI) kg C m⁻². In contrast, soil C concentrations in the lawn
337 increased only 25% from 3.92 ([3.00, 5.02] 95%CI) to 4.91 ([3.29, 7.25] 95%CI) kg C m⁻² (Fig.
338 3), which was not significantly different. The original soil strata beneath the UFF sequestered
339 slightly more C than corresponding areas of the lawn (UFF original soil C sequestration = 0.77
340 ([0.22,1.72] 95%CI) kg m⁻² y⁻¹; Lawn soil C sequestration = 0.49 ([0.14,1.11] 95%CI kg m⁻² y⁻¹),
341 while the vast majority of C was sequestered in the berm stratum (3.35 ([1.38,6.56] 95%CI) kg
342 m⁻² y⁻¹).

343



344
 345 **Fig. 3** Soil carbon density approximately doubled in the Urban Food Forest compared to a
 346 negligible increase in the lawn. Error bars represent posterior 95% credible intervals for each
 347 stratum and area. Dark fill corresponds to carbon concentration within the berm stratum of the
 348 Urban Food Forest. Medium fill corresponds to carbon concentration in the original upper
 349 stratum of soil in either area (0-10 cm depth). Light fill corresponds to the original lower soil
 350 stratum in either area (10-20 cm depth).

351 While differences between areas demonstrated how quickly UFF adds SOC, fine scale
352 variation within the UFF indicated approaching limits to its SOC sequestration capacity.
353 Contrary to our expectation that different tree functional traits would exaggerate fine-scale
354 variation in C sequestration, C densities became more homogenous because locations that began
355 with relatively high SOC sequestered less C than locations with relatively low initial SOC (Fig.
356 4A). The negative linear relationship between initial SOC stocks and SOC sequestration is
357 consistent with a simple soil C mass balance model (Eq. 1). After parameterizing the model from
358 spatially detrended C stock and sequestration values, the SOC supply rate was estimated as 6.57
359 $\text{kg C m}^{-2} \text{yr}^{-1}$ ([3.73, 10.9] 95%CI) and the SOC mineralization rate was estimated as 0.41 yr^{-1}
360 ([0.04, 0.70] 95%CI). Meeting the estimated SOC supply rate from added mulch alone would
361 have required 13.2 $\text{kg C m}^{-2} \text{yr}^{-1}$ ([7.46, 21.9] 95%CI) corresponding to a layer 6.6 cm deep
362 converted directly into soil C each year. Given the estimated SOC supply and mineralization
363 rates, the mass balance equation projected an equilibrium SOC stock of 14.48 kg C m^{-2} ([8.94,
364 19.02] 95%CI). After just two years, the UFF had attained nearly 90% of its estimated SOC
365 stock capacity and was projected to achieve 95% of its capacity after only 4 years. By contrast,
366 the estimated SOC supply rate in the lawn was significantly lower than in the UFF, 2.56
367 ([1.63,3.87] 95%CI) $\text{kg C m}^{-2} \text{yr}^{-1}$ with a slightly higher mineralization rate (0.526 [0.41,0.67]
368 95%CI yr^{-1}) and was within 1% of its estimated equilibrium, 4.88 ([3.31,7.20] 95% CI) kg C m^{-2}
369 (Figure S3), which aligns with our statistically insignificant estimated increase in SOC.
370



371
 372 **Fig. 4** Fine scale changes in soil carbon concentration over two years implies that the Urban
 373 Food Forest exhibits system-level mass balance (a) and a rapidly approaching limit to
 374 sequestration capacity (b). Transparent line overlay represents 1200 draws from the posterior
 375 distribution for the estimated SOC supply rate (K) and mineralization rate (α) parameters (Eq. 1).

376 **Discussion**

377 Established ecological theory (Loreau 2010; Hulvey et al. 2013) and emerging empirical
378 syntheses (Feliciano et al. 2018; Salbitano et al. 2019) agree with policy analysis (McElwee et al.
379 2020) that replacing unproductive urban land uses with UFF can mitigate related problems of
380 urban food security and climate change. Only two years after converting lawn to UFF, our land
381 use experiment demonstrated agriculturally relevant improvements in multiple dimensions of soil
382 function with especially rapid soil C sequestration. However, fine-scale changes in C stocks
383 generated more uniform conditions, despite the high diversity of tree species involved, implying
384 that system level constraints have rapidly emerged in the UFF. Comparing our results to existing
385 analyses of urban agriculture and agroforestry contextualizes the promise and limitations of UFF
386 as a sustainable solution to major environmental challenges.

387 *UFF improves soil function*

388 Soil compaction, whereby stress from mechanical loads reduces soil pore space and
389 associated biological functions, is the most widespread and important physical means for soil
390 degradation in urbanized and agricultural soils (Nawaz et al. 2013; Smith et al. 2016; Thompson
391 and Kao-Kniffin 2019). Natural recovery can take decades of physical cycling and
392 bioperturbation (Nawaz et al. 2013). However, we found rapid decompaction following land use
393 change, as measured by significant differences in SBD between the same soil strata under the
394 UFF and at control sites in the lawn. The magnitude of change was similar to that reported in
395 other recent studies of land use change. Two years after converting vacant lots in Ohio, U.S.A. to
396 vegetable gardens, surface SBD decreased from 1.79 g cm⁻³ to 0.98 g cm⁻³ (Beniston et al. 2016),
397 a change approximately 11% greater than what we observed. Rapid soil decompaction in the
398 UFF without direct mechanical perturbation probably reflects a combination of processes,

399 including exclusion of heavy lawn mowers, increased woody root growth and infiltration of
400 organic matter produced *in situ* and added with management.

401 Converting lawn to UFF also improved biological and chemical metrics for soil function.
402 Soil activity, as measured by short-term respiration, was significantly higher in both the imported
403 berm soil and original topsoil than it was in the topsoil of the lawn. Similar increases in soil
404 respiration have been documented close to established trees in both experiments and
405 observations of agroforestry systems (Lee and Jose 2003; Hoosbeek et al. 2018). We note that
406 the short duration of our *ex situ* measurements exclude soil C efflux from more recalcitrant
407 compounds and root respiration. Longer incubations and *in situ* measurements would be
408 necessary to estimate ecosystem-level soil C efflux in a way that is comparable to the
409 mineralization rates that we estimated using the mass balance model (Eq. 1).

410 Higher soil activity tends to increase nutrient availability (Van Der Heijden et al. 2008),
411 which is consistent with the higher nutrient concentrations and CEC that we measured in the
412 UFF compared to the lawn. In the control lawn area, leaf clippings were retained, which tends to
413 increase nutrient availability and SOC storage relative to management that removes clippings
414 (Thompson and Kao-Kniffin 2019), but lawn management did not add fertilizer. Some of the
415 improvement in soil activity and nutrient availability in the UFF could directly reflect input from
416 compost, which was instrumental in improving C stocks in experimental reforestation plots in
417 New York City (Ward et al. 2021). However, a forest garden in France without exogenous inputs
418 exhibited higher CEC and nutrient availability than conventional agricultural soils, likely
419 because tree roots improved mineral weathering and plant litter retained nutrients within the
420 system (de Tombeur et al. 2018). Determining whether improved soil chemistry sustainably

421 increases yields will require more detailed analysis of soil nutrient speciation as well as an
422 assessment of nutrient losses with harvest compared to input from exogenous sources.

423 Improvements in both soil activity and nutrient availability coincided with the
424 development of a more diverse and functionally distinctive soil microbial community in the UFF
425 compared to the lawn. The differences that we observed may combine the known beneficial
426 effects of both agroforestry and urban agriculture. Converting forests to agriculture generally
427 decreases the diversity of soil bacteria, which recovers following reforestation (Díaz-Vallejo et
428 al. 2021). These changes can have important functional consequences. Compared to farmland,
429 agroforestry systems in China had higher soil C and respiration, which correlated with increased
430 diversity of both bacteria and fungi (Ren et al. 2018). The increases in bacteria were also
431 associated with changes in nutrient composition (Ren et al. 2018). Urbanization also impacts soil
432 microbial community structure and function, such that urban soils tend to have reduced bacterial
433 biomass and diversity (Guilland et al. 2018). However, microbial diversity within urban
434 greenspaces varies greatly depending on cultivation and the presence of woody plants
435 (Thompson and Kao-Kniffin 2019). In Adelaide, Australia, nutrient availability and bacterial
436 richness were highest in urban garden plots and much lower in lawns of sports fields (Baruch et
437 al. 2021). Sports fields also had lower fungal richness, particularly among saprotrophic taxa,
438 compared to urban greenspaces with woody vegetation (Baruch et al. 2020). Taken together with
439 our analysis, these results strongly suggest that cultivating diverse woody plant species in urban
440 settings changes microbial communities in ways that promote physical and chemical dimensions
441 of soil function relative to traditionally managed lawn.

442 *Rapid SOC sequestration exhibits system-level constraints*

443 Gains in soil function coincided with rapid SOC sequestration, reinforcing the potential
444 for urban land use to mitigate climate change. While lawns can store more SOC than other land
445 covers, depending on their management and biogeography (Thompson and Kao-Kniffin 2019),
446 we measured relatively low SOC concentrations (4.91 kg C m^{-2}) that were nearly identical to
447 those measured in urban lawns in another region of Florida (4.9 kg C m^{-2} , Nagy et al. (2014)).
448 Moreover, lawn SOC did not significantly increase after two years, implying that 70 years of
449 consistent management generated an SOC equilibrium, as has been documented after just 30
450 years in other urban grasslands (Shi et al. 2012). Compared to the relatively low equilibrium
451 SOC concentrations in the lawn, establishing the UFF precipitated a dramatic increase in SOC.
452 The magnitude was high but within the range observed for certain agroforestry systems. An early
453 modelling analysis estimated potential soil C sequestration of up to 23 kg m^{-2} by converting
454 traditional agriculture to agroforestry (Albrecht and Kandji 2003), which is consistent with
455 empirical measurements from Canada which found over 20.1 kg C m^{-2} in soils from forested
456 sites compared to just 15 kg C m^{-2} in herblands (Baah-Acheamfour et al. 2015). The comparable
457 land cover types in our study showed a similar difference in surface SOC stocks. Our
458 measurements were also similar to values reported from coffee polyculture in Costa Rica (16.8
459 kg C m^{-2} , Alpizar et al., 1986), which is very similar to the maximum attainable SOC that we
460 projected of approximately 16 kg C m^{-2} . Our measurements differ from others primarily due to
461 the rapid initial rate of sequestration in berm soils ($3.35 \text{ kg C m}^{-2} \text{ yr}^{-1}$), which was nearly five
462 times faster than observed in most agroforestry systems (Feliciano et al. 2018). However, the rate
463 of C sequestration that we observed in the original upper stratum of soil ($0.77 \text{ kg m}^{-2} \text{ y}^{-1}$) is much
464 closer to values reported from other agroforestry systems.

465 Several factors could contribute to the high values for SOC stocks and sequestration that
466 we observed in our study. First, our measurements occurred along berms where soil amendments
467 and tree plantings were concentrated. Because SOC concentrations tend to increase closer to
468 trees (Cardinael et al. 2020; Clivot et al. 2020), our values represent a maximum SOC stock for a
469 subset of the UFF soils. Additional sampling from intervening alleys would more accurately
470 estimate the SOC stocks of the entire project area and would probably yield lower average SOC
471 concentrations that are closer to values that have been reported for other agroforestry
472 experiments. Geographic and biological factors could also contribute to the high maximum
473 values for SOC concentrations that we observed. Agroforestry projects in warmer locations tend
474 to exhibit higher soil C concentrations (Feliciano et al. 2018). Also, ecological theory and
475 experiments indicate that increasing woody plant diversity and associated functional trait
476 variation tends to increase SOC sequestration (Hulvey et al. 2013). Our experiment included 33
477 species of trees and many more perennial pseudowoodly herbs, vines and grasses with contrasting
478 biogeographic origins. The extreme functional diversity of species involved could have increased
479 the maximum SOC concentration. Additional experiments that vary species composition across
480 climatic gradients are necessary to estimate how and why the SOC capacity of UFF may vary
481 from other land use types.

482 While maximum SOC stocks and sequestration rates that we estimated were high, fine-
483 scale variability implied a rapidly approaching limit to SOC sequestration. Contrary to our
484 prediction that contrasting tree functional traits would exaggerate initial differences in SOC
485 concentrations, with some species storing more C belowground than others, fine-scale variability
486 in SOC concentrations actually decreased through time. The negative correlation between initial
487 SOC concentration and subsequent SOC sequestration was consistent with a mass balance model

488 (Eq. 1). The model, which has been used to estimate SOC capacity for global land cover types
489 (Morais et al. 2019), is considerably simpler than widely used mechanistic models for soil C
490 cycling (e.g. CENTURY, Parton et al. 1988; RothC, Coleman et al. 1997), and assumes uniform
491 conditions with constant SOC supply and proportionally constant mineralization. Our finding
492 that these assumptions approximately hold in a two-year old land use experiment has two major
493 implications.

494 The first implication is that the system has fixed C sequestration capacity under current
495 management and biological conditions. Indeed, 90% of attainable SOC had been reached just
496 two years after establishment. For this reason, UFF soils may quickly meet discrete C
497 sequestration goals, for instance as carbon credits, but not for mitigating ongoing emissions. It is
498 possible that succession above and belowground could alter the parameters of the mass balance
499 model to change the equilibrium SOC concentration or break the assumptions of the model
500 altogether such that ongoing SOC sequestration is more likely. A recent metanalysis indicated
501 that agroforestry soil C sequestration rates may be multiphasic, with an initial decelerating trend
502 yielding to a transitory increase before a long term steady state (Feliciano et al. 2018). For a
503 holistic picture of how UFF can factor into mitigation schemes, further measurements and
504 modelling will be necessary to estimate the capacity and rate of C sequestration aboveground,
505 which are reported to be considerable (Schafer et al. 2019), as well as the extent to which local
506 food production offsets GHG emissions as has been demonstrated for other forms of urban
507 agriculture (Cleveland et al. 2017).

508 The second major implication is that converting lawn to UFF precipitated the emergence
509 of system-level regulation in just two years. Exogenous and endogenous factors could contribute.
510 Added compost and mulch supply SOC and could homogenize microbial communities in a way

511 that promotes constant proportional mineralization. The mass balance model constrains the
512 quantity of exogenous inputs necessary to explain the increase in UFF SOC concentrations.
513 Assuming that mulch was the main exogenous source of SOC during establishment, several tons
514 added per year would be necessary to account for all of the additional C, which is inconsistent
515 with the management history of the site. However, differences in management intensity and
516 duration certainly contributed to the differences in stocks and sequestration between the UFF and
517 the lawn. The lawn received neither irrigation nor fertilizer, which tend to increase SOC
518 concentrations and sequestration (Thompson and Kao-Kniffin 2019). Elsewhere in Florida,
519 where lawns likely received more inputs and urban forests, less, differences in soil SOC
520 concentrations between these two land covers were not significantly different (Nagy et al. 2014).
521 Given that short term changes in management can modify long-term equilibrium conditions in
522 both lawns and forests (Peach et al. 2019), strategic use of irrigation and fertilizers may increase
523 soil function and carbon sequestration across a range of urban land covers

524 While management may contribute to system-level regulation in both lawn and UFF, the
525 speed with which it emerged in the UFF despite the extreme functional diversity of plants raises
526 the possibility that endogenous mechanisms played some role. The community of woody plants
527 and associated organisms, including people, may reinforce negative feedback regulation over
528 belowground C cycling at the system-level. For example, shared mycorrhizal networks can
529 redistribute photosynthetic resources to reduce variation in resource stress among trees in forests
530 (Klein et al. 2016). Analogous exchanges involving SOC supply and mineralization may operate
531 within the UFF. In other words, from the perspective of soil C cycling, the collection of plants
532 under current management began to behave like a forest. As such, soil C mass balance could
533 serve as an objective criterion for delineating forest ecosystems independent of arbitrary

534 definitions that depend on tree stem density and size distributions. Identifying which
535 mechanisms generate this pattern, as well as their characteristic temporal and spatial scales,
536 could be a productive avenue for basic and applied research on C cycling and sequestration in
537 forest ecosystems.

538 **Declaration**

539 **Ethics approval:** Not applicable

540 **Competing Interests:** The authors have no relevant financial or non-financial competing
541 interests to disclose.

542 **Funding:** New College of Florida students funded the land use experiment through the New
543 College of Florida Green Fee. Additional funds for soil analyses were provided by the New
544 College of Florida Foundation.

545 **Availability of data and material:** All data necessary to reproduce the analysis will be made
546 available upon acceptance of the manuscript. Code is provided in Supplementary Information.

547 **Author Contributions:** All authors contributed to the study conception and design. Material
548 preparation and data collection were performed by Jay McWilliams and Steven Bressan. Data
549 analysis was conducted by Brad Oberle and Erika Díaz-Almeyda. The first draft of the
550 manuscript was written by Brad Oberle. All authors commented on previous versions of the
551 manuscript. All authors read and approved the final manuscript.

552 **References**

- 553 Albrecht A, Kandji ST (2003) Carbon sequestration in tropical agroforestry systems. *Agric*
554 *Ecosyst Environ* 99:15–27. [https://doi.org/10.1016/S0167-8809\(03\)00138-5](https://doi.org/10.1016/S0167-8809(03)00138-5)
- 555 Alpizar L, Fassbender HW, Heuvelop J, et al (1986) Modelling agroforestry systems of cacao (*Theobroma cacao*) with laurel (*Cordia alliodora*) and poro (*Erythrina poeppigiana*).
556 *Agrofor Syst* 175–189
- 557
- 558 Baah-Acheamfour M, Chang SX, Carlyle CN, Bork EW (2015) Carbon pool size and stability
559 are affected by trees and grassland cover types within agroforestry systems of western
560 Canada. *Agric Ecosyst Environ* 213:105–113. <https://doi.org/10.1016/j.agee.2015.07.016>
- 561 Baruch Z, Liddicoat C, Cando-Dumancela C, et al (2021) Increased plant species richness
562 associates with greater soil bacterial diversity in urban green spaces. *Environ Res*
563 196:110425. <https://doi.org/10.1016/j.envres.2020.110425>
- 564 Baruch Z, Liddicoat C, Laws M, et al (2020) Characterising the soil fungal microbiome in
565 metropolitan green spaces across a vegetation biodiversity gradient. *Fungal Ecol* 47:100939.
566 <https://doi.org/10.1016/j.funeco.2020.100939>
- 567 Beniston JW, Lal R, Mercer KL (2016) Assessing and Managing Soil Quality for Urban
568 Agriculture in a Degraded Vacant Lot Soil. *L Degrad Dev* 27:996–1006.
569 <https://doi.org/10.1002/ldr.2342>
- 570 Cardinael R, Chevallier T, Guenet B, et al (2020) Organic carbon decomposition rates with depth
571 and contribution of inorganic carbon to CO₂ emissions under a Mediterranean agroforestry
572 system. *Eur J Soil Sci* 71:909–923. <https://doi.org/10.1111/ejss.12908>
- 573 Cardoso EJBN, Vasconcellos RLF, Bini D, et al (2013) Soil health: Looking for suitable
574 indicators. What should be considered to assess the effects of use and management on soil

- 575 health? *Sci Agric* 70:274–289. <https://doi.org/10.1590/S0103-90162013000400009>Clark
576 KH, Nicholas KA (2013) Introducing urban food forestry: A multifunctional approach to
577 increase food security and provide ecosystem services. *Landsc Ecol* 28:1649–1669.
578 <https://doi.org/10.1007/s10980-013-9903-z>
- 579 Cleveland DA, Phares N, Nightingale KD, et al (2017) The potential for urban household
580 vegetable gardens to reduce greenhouse gas emissions. *Landsc Urban Plan* 157:365–374.
581 <https://doi.org/10.1016/j.landurbplan.2016.07.008>
- 582 Clivot H, Petitjean C, Marron N, et al (2020) Early effects of temperate agroforestry practices on
583 soil organic matter and microbial enzyme activity. *Plant Soil* 453:189–207.
584 <https://doi.org/10.1007/s11104-019-04320-6>
- 585 Coleman K, Jenkinson DS, Crocker GJ, et al (1997) Simulating trends in soil organic carbon in
586 long-term experiments using RothC-26.3. *Geoderma* 81: [https://doi.org/10.1016/S0016-](https://doi.org/10.1016/S0016-7061(97)00079-7)
587 [7061\(97\)00079-7](https://doi.org/10.1016/S0016-7061(97)00079-7)
- 588 Conner MM, Saunders WC, Bouwes N, Jordan C (2015) Evaluating impacts using a BACI
589 design, ratios, and a Bayesian approach with a focus on restoration. *Environ Monit Assess*
590 188: <https://doi.org/10.1007/s10661-016-5526-6>
- 591 De Cáceres M, Legendre P (2020) Package “indicpecies.” CRAN Repos
- 592 De Stefano A, Jacobson MG (2018) Soil carbon sequestration in agroforestry systems: a meta-
593 analysis. *Agrofor Syst* 92:285–299. <https://doi.org/10.1007/s10457-017-0147-9>
- 594 de Tombeur F, Sohy V, Chenu C, et al (2018) Effects of permaculture practices on soil
595 physicochemical properties and organic matter distribution in aggregates: A case study of
596 the bec-hellouin farm (France). *Front Environ Sci* 6:1–12.
597 <https://doi.org/10.3389/fenvs.2018.00116>

- 598 Díaz-Vallejo EJ, Seeley M, Smith AP, Marín-Spiotta E (2021) A meta-analysis of tropical land-
599 use change effects on the soil microbiome: Emerging patterns and knowledge gaps.
600 *Biotropica* 53 <https://doi.org/10.1111/btp.12931>
- 601 Dowd SE, Sun Y, Wolcott RD, Domingo A, Carroll JA (2008) Bacterial tag–encoded FLX
602 amplicon pyrosequencing (bTEFAP) for microbiome studies: bacterial diversity in the
603 ileum of newly weaned *Salmonella*-infected pigs. *Foodborne Pathog Dis* 5: 459–472
604 [10.1089/fpd.2008.0107](https://doi.org/10.1089/fpd.2008.0107)
- 605 Feliciano D, Ledo A, Hillier J, Nayak DR (2018) Which agroforestry options give the greatest
606 soil and above ground carbon benefits in different world regions? *Agric Ecosyst Environ*
607 254:117–129. <https://doi.org/10.1016/j.agee.2017.11.032>
- 608 Forest Products Laboratory (2010) *Wood Handbook: Wood as an Engineering Material*.
609 *Agriculture* 72:466. <https://doi.org/10.1093/gtra/190>
- 610 Guillard C, Maron PA, Damas O, Ranjard L (2018) Biodiversity of urban soils for sustainable
611 cities. *Environ Chem Lett* 16:1267–1282. <https://doi.org/10.1007/s10311-018-0751-6>
- 612 Hackl E, Zechmeister-Boltenstern S, Bodrossy L, Sessitsch A (2004) Comparison of diversities
613 and compositions of bacterial populations inhabiting natural forest soils. *Appl Environ*
614 *Microbiol* 70:5057–5065. <https://doi.org/10.1128/AEM.70.9.5057-5065.2004>
- 615 Hoosbeek MR, Remme RP, Rusch GM (2018) Trees enhance soil carbon sequestration and
616 nutrient cycling in a silvopastoral system in south-western Nicaragua. *Agrofor Syst* 92:263–
617 273. <https://doi.org/10.1007/s10457-016-0049-2>
- 618 Hulvey KB, Hobbs RJ, Standish RJ, et al (2013) Benefits of tree mixes in carbon plantings. *Nat*
619 *Clim Chang* 3:869–874. <https://doi.org/10.1038/nclimate1862>
- 620 Huang, JW, Hu, SL, Cheng, XK, Chen, D, Kong, XK, Jiang, JD (2019) *Steroidobacter soli* sp.

- 621 nov., isolated from farmland soil. *Int J Syst Evol Microbiol* 69:3443–3447.
622 <https://doi.org/10.1099/ijsem.0.003639>
- 623 Klein T, Siegwolf RTW, Körner C (2016) Belowground carbon trade among tall trees in a
624 temperate forest. *Science* 352: <https://doi.org/10.1126/science.aad6188>
- 625 Lee KH, Jose S (2003) Soil respiration and microbial biomass in a pecan - Cotton alley cropping
626 system in southern USA. *Agrofor Syst* 58:45–54. <https://doi.org/10.1023/A:1025404019211>
- 627 Loreau M (2010) Linking biodiversity and ecosystems: towards a unifying ecological theory.
628 *Philos Trans R Soc Lond B Biol Sci* 365:49–60. <https://doi.org/10.1098/rstb.2009.0155>
- 629 McDougall R, Kristiansen P, Rader R (2019) Small-scale urban agriculture results in high yields
630 but requires judicious management of inputs to achieve sustainability. *Proc Natl Acad Sci U*
631 *S A* 116:129–134. <https://doi.org/10.1073/pnas.1809707115>
- 632 McElwee P, Calvin K, Campbell D, et al (2020) The impact of interventions in the global land
633 and agri-food sectors on Nature’s Contributions to People and the UN Sustainable
634 Development Goals. *Glob Chang Biol* 26:4691–4721. <https://doi.org/10.1111/gcb.15219>
- 635 McMurdie PJ, Holmes S (2013) Phyloseq: An R Package for Reproducible Interactive Analysis
636 and Graphics of Microbiome Census Data. *PLoS One* 8:
637 <https://doi.org/10.1371/journal.pone.0061217>
- 638 Morais TG, Teixeira RFM, Domingos T (2019) Detailed global modelling of soil organic carbon
639 in cropland, grassland and forest soils. *PLoS One* 14
640 <https://doi.org/10.1371/journal.pone.0222604>
- 641 Nagy R, Lockaby BG, Zipperer WC, Marzen LJ (2014). A comparison of carbon and nitrogen
642 stocks among land uses/covers in coastal Florida. *Urban Ecosyst* 17:255–276. DOI
643 10.1007/s11252-013-0312-5

- 644 Nawaz MF, Bourrié G, Trolard F (2013) Soil compaction impact and modelling. A review.
645 *Agron Sustain Dev* 33:291–309. <https://doi.org/10.1007/s13593-011-0071-8>
- 646 Nguyen NH, Song Z, Bates ST, et al (2016) FUNGuild: An open annotation tool for parsing
647 fungal community datasets by ecological guild. *Fungal Ecol* 20:
648 <https://doi.org/10.1016/j.funeco.2015.06.006>
- 649 Nytofte JLS, Henriksen CB (2019) Sustainable food production in a temperate climate – a case
650 study analysis of the nutritional yield in a peri-urban food forest. *Urban For Urban Green*
651 45: <https://doi.org/10.1016/j.ufug.2019.04.009>
- 652 Ogle K, Barber JJ (2012) Bayesian Statistics. In: Hastings A, Gross L (eds) *Sourcebook in*
653 *Theoretical Ecology*. University of California Press, Berkeley
- 654 Parada AE, Needham DM, Fuhrman JA (2016) Every base matters: assessing small subunit
655 rRNA primers for marine microbiomes with mock communities, time series and global field
656 samples. *Environ Microbiol* 18: 1403-1414
- 657 Parton WJ, Stewart JWB, Cole C V. (1988) Dynamics of C, N, P and S in grassland soils: a
658 model. *Biogeochemistry* 5:109–131
- 659 Peach ME, Ogden LA, Mora EA, Friedland AJ (2019). Building houses and managing lawns
660 could limit yard soil carbon for centuries. *Carbon Balance Manage* 14:1–14
661 <https://doi.org/10.1186/s13021-019-0124-x>
- 662 R Core Team (2020) R software: Version 4.0.2. R Found Stat Comput
- 663 Ren C, Wang T, Xu Y, et al (2018) Differential soil microbial community responses to the
664 linkage of soil organic carbon fractions with respiration across land-use changes. *For Ecol*
665 *Manage* 409:170–178. <https://doi.org/10.1016/j.foreco.2017.11.011>
- 666 Salbitano F, Fini A, Borelli S, Konijnendijk CC (2019) Editorial - Urban Food Forestry: Current

- 667 state and future perspectives. *Urban For Urban Green* 45
668 <https://doi.org/10.1016/j.ufug.2019.126482>
- 669 Schafer LJ, Lysák M, Henriksen CB (2019) Tree layer carbon stock quantification in a temperate
670 food forest: A peri-urban polyculture case study. *Urban For Urban Green* 45:126466.
671 <https://doi.org/10.1016/j.ufug.2019.126466>
- 672 Shi W, Bowman D, Rufty (2012) Microbial control of soil carbon accumulation in turfgrass
673 systems. In: Lal R, Augustin B (eds) *Carbon Sequestration in Urban Ecosystems*. Springer,
674 Dordrecht, pp 215–231. 10.1007/978-94-007-2366-5_11
- 675 Smith P, House JI, Bustamante M, et al (2016) Global change pressures on soils from land use
676 and management. *Glob Chang Biol* 22:1008–1028. <https://doi.org/10.1111/gcb.13068>
- 677 Sparkman J, Bryant J (2016) New College of Florida campus master plan.
678 [https://www.ncf.edu/wp-content/uploads/2020/08/NCF-Masterplan_Amendment-1_August-](https://www.ncf.edu/wp-content/uploads/2020/08/NCF-Masterplan_Amendment-1_August-2016.pdf)
679 [2016.pdf](https://www.ncf.edu/wp-content/uploads/2020/08/NCF-Masterplan_Amendment-1_August-2016.pdf) 1/7/2023. Accessed 17 January 2023
- 680 Soil Science Division Staff (2017) *Soil survey manual*. Ditzler C, Scheffe K, Monger HC (eds)
681 USDA Handbook 18. Government Printing Office, Washington
- 682 Soil Survey Staff (2023) *Soil Series Classification Database*. Natural Resources Conservation
683 Service, USDA. <https://data.nal.usda.gov/dataset/soil-series-classification-database-sc>.
684 Accessed 17 January 2023
- 685 Tang, YL, Lin, HP, Xie, QY, Li, L, Peng, F, Deng, Z, Hong, K (2013) *Actinoallomurus*
686 *acanthiterrae* sp. nov., an actinomycete isolated from rhizosphere soil of the mangrove plant
687 *Acanthus ilicifolius*. *Int J Syst Evol Microbiol* 63:1874–1879.
688 <https://doi.org/10.1099/ijs.0.043380-0>
- 689 Thompson GL, Kao-Kniffin J (2019) Urban grassland management implications for soil C and N

- 690 dynamics: a microbial perspective. *Front Ecol Evol* 7
691 <https://doi.org/10.3389/fevo.2019.00315>
- 692 Trumbore S (2000) Age of soil organic matter and soil respiration: Radiocarbon constraints on
693 belowground C dynamics. *Ecol Appl* 10: [https://doi.org/10.1890/1051-](https://doi.org/10.1890/1051-0761(2000)010[0399:AOSOMA]2.0.CO;2)
694 [0761\(2000\)010\[0399:AOSOMA\]2.0.CO;2](https://doi.org/10.1890/1051-0761(2000)010[0399:AOSOMA]2.0.CO;2)
- 695 USDA (1948) Aerial photographs of Sarasota County - Flight 1D (1948)
696 <http://ufdc.ufl.edu/UF00071781/00001> Accessed 17 January 2023
- 697 USDA (2011) U.S. Agriculture and Forestry Greenhouse Gas Inventory: 1990-2008. Hohenstein
698 W (ed) Technical Bulletin 1930
- 699 Van Der Heijden MGA, Bardgett RD, Van Straalen NM (2008) The unseen majority: Soil
700 microbes as drivers of plant diversity and productivity in terrestrial ecosystems. *Ecol Lett*
701 11:296–310. <https://doi.org/10.1111/j.1461-0248.2007.01139.x>
- 702 Walkley A, Black IA (1934) An examination of the degtjareff method for determining soil
703 organic matter, and a proposed modification of the chromic acid titration method. *Soil Sci*
704 37 <https://doi.org/10.1097/00010694-193401000-00003>
- 705 Ward EB, Doroski DA, Felson AJ, et al (2021) Positive long-term impacts of restoration on soils
706 in an experimental urban forest. *Ecol Appl* 31:1–15. <https://doi.org/10.1002/eap.2336>
- 707 White TJ, Bruns T, Lee SJWT, Taylor J (1990). Amplification and direct sequencing of fungal
708 ribosomal RNA genes for phylogenetics. In: Innis MA, Gelfand DH, Sninsky JJ, White TJ
709 (eds) *PCR protocols: a guide to methods and applications*, Academic Press, San Diego, pp
710 315-322

711 **Supplementary Information Caption:**

712 This article includes Supplementary Information

713 **Table S1** Inventory of woody species plantings

714 **Table S2** Sampling strategy

715 **Table S3** Information theoretic criteria (Akaike Information Criterion, AIC) for alternative
716 regression relationships in calibration dataset. Models compare both Organic Carbon (OC) and
717 Soil Bulk Density (SBD), against explanatory factors, Area and Stratum, and Loss-on-Ignition
718 (LOI). Most adequate models correspond to lowest AIC and are highlighted in bold.

719 **Table S4 A:** Heat map of fungal OTU relative abundance for the most dominant taxa identified
720 in four soil samples from UFF and two from Lawn.

721 **Table S4 B:** Heat map of bacterial OTU relative abundance for the most dominant taxa
722 identified in four soil samples from UFF and two from Lawn.

723 **Figure S1:** Aerial imagery of land cover at the study site in 1948 (a) and 2019 (b) with the study
724 area footprint approximately represented by opposed trapezoids, with the UFF and lawn north
725 and south, respectively, of the contemporary roadway. The scale bars are approximately 150 m
726 long and north is vertical as depicted. Historical aerial imagery available at

727 <http://ufdc.ufl.edu/UF00071781/00001> accessed 17 January 2023. Contemporary aerial imagery
728 provided by Landsat available at <https://landsat.visibleearth.nasa.gov/> accessed 17 January 2023.

729 **Figure S2:** Calibration relationships between $\ln(\text{Loss-on-Ignition})$ and both $\ln(\text{Organic Carbon})$
730 (a) and $\ln(\text{Soil bulk density})$ (b) among 15 samples representing low, high and intermediate LOI
731 samples from each area and stratum.

732 **Figure S3:** Fine scale changes in soil carbon concentration over two years in the lawn is
733 consistent with mass balance (A) and is close to equilibrium (B). Transparent line overlay

734 represents 1200 draws from the posterior distribution for the estimated SOC supply rate (K) and
735 mineralization rate (α) parameters (Eq. 1).

736 **Supplementary Methods:** Detailed description of the hierarchical Bayesian statistical model.

737 **Supplementary Code:** Annotated code for R statistical computing environment necessary to
738 reproduce all results and figures.

739